Supporting Information for

Tetraalkylammonium salts of platinum nitratocomplexes: isolation, structure and relevance to the preparation of PtO_x/CeO_2 catalysts for low-temperature CO oxidation.

Danila Vasilchenko[a,b*], Polina Topchiyan[a,b], Semen Berdyugin[a], Evgeny Filatov[a,c], Sergey Tkachev[a], Iraida Baidina[a], Vladislav Komarov[a,c], Elena Slavinskaya[b], Andrey Stadnichenko[b,c], Evgeny Gerasimov[b,c]

[a]*Nikolaev Institute of Inorganic Chemistry, Siberian Branch of the Russian Academy of Science, 630090 Novosibirsk, Russian Federation*

[b]*Novosibirsk State University, 630090 Novosibirsk, Russian Federation*

[c]*Boreskov Institute of Catalysis 630090 Novosibirsk, Russia*

*e-mail: vasilchenko@niic.nsc.ru

Table S1. Crystal data and structure refinement parameters for compounds **2**, **3a**, **3b** and **4**.

Compounds	**2**	**3b**	**3a**	**4**
Stoichiometric formula	$C_8H_{21}N_5O_{13}Pt$	$C_{24}H_{58}N_{10}O_{26}Pt_2$	$C_{24}H_{56}N_8O_{18}Pt$	$C_{32}H_{72}N_8O_{18}Pt$
Formula weight	590.39	1292.98	939.86	1052.07
Temperature (K)	240(2) K	150(2)	150(2)	296(2)
Wavelength (Å)	1.54178	0.71073	0.71073	0.71073
Crystal system	Triclinic	Monoclinic	Triclinic	Monoclinic
Space group	P-1	C2/c	P-1	$P2_1/n$
Unit cell dimensions (Å, °)	a = 9.4977(8) α = 114.284(2)	a = 17.832(1) α = 90	a = 9.6283(4) α = 115.660(1)	a = 10.9021(9) α = 90
	b = 10.0974(8) β = 94.929(3)	b = 18.999(1) β = 116.944(3)	b = 10.9803(5) β = 103.271(1)	b = 15.659(1) β = 91.991(2)
	c = 10.7125(9) γ = 92.338(3)	c = 14.801(1) γ = 90	c = 11.4179(4) γ = 103.642(2)	c = 13.669(1) γ = 90
Volume ($Å^3$), Z	929.7(1),2	4470.1(6),4	978.64(7), 1	2332.1(3), 2
Absorption coefficient (mm^{-1})	14.833	6.349	3.664	3.084
D_{calc} ($g \cdot cm^{-3}$)	2.109	1.921	1.595	1.498
F(000)	572	2544	478	1084
θ range for data collection (°)	4.69 - 67.74	2.56 - 29.16	2.14 - 25.80	2.28 - 30.62
Limiting indices	-11 ≤ **h** ≤ 11	-25 ≤ **h** ≤ 25	-11 ≤ **h** ≤ 11	-15 ≤ **h** ≤ 15
	-12 ≤ **k** ≤ 12	-27 ≤ **k** ≤ 27	-12 ≤ **k** ≤ 13	-22 ≤ **k** ≤ 21
	-12 ≤ **l** ≤ 12	-21 ≤ **l** ≤ 21	-13 ≤ **l** ≤ 9	-19 ≤ **l** ≤ 17
Reflections collected	16730	38781	9593	34111
Independent reflections	3328 [R(int) = 0.0346]	6609 [R(int) = 0.0319]	3737 [R(int) = 0.0218]	7135 [R(int) = 0.0210]
Completeness (%)	99.1	98.2	99.6	99.9
Max. and min. transmission	0.5242 and 0.2306	0.5988 and 0.2147	0.4269 and 0.6676	0.6098 and 0.4673
Refinement method	Full-matrix least-squares on F^2			
Data / constraints / parameters	3328 / 1 / 249	6880/ 14 / 319	3737 / 0 / 236	7135 / 0 / 272
Goodness-of-fit on F^2	1.054	1.095	1.088	1.116
Final R indices [$I > 2\sigma(I)$]	R1 = 0.0203, wR2 = 0.0506	R1 = 0.0313, wR2 = 0.0752	R1 = 0.0147, wR2 = 0.0332	R1 = 0.0223, wR2 = 0.0529
R indices (all data)	R1 = 0.0208, wR2 = 0.0509	R1 = 0.0435, wR2 = 0.0789	R1 = 0.0147, wR2 = 0.0332	R1 = 0.0370, wR2 = 0.0567
Largest diff. peak/hole, $e \cdot Å^{-3}$	0.700 / -0.811	3.596 / -2.268	0.474 / -0.441	2.089 / -0.506
CCDC №	1891138	1891136	1891135	1891139

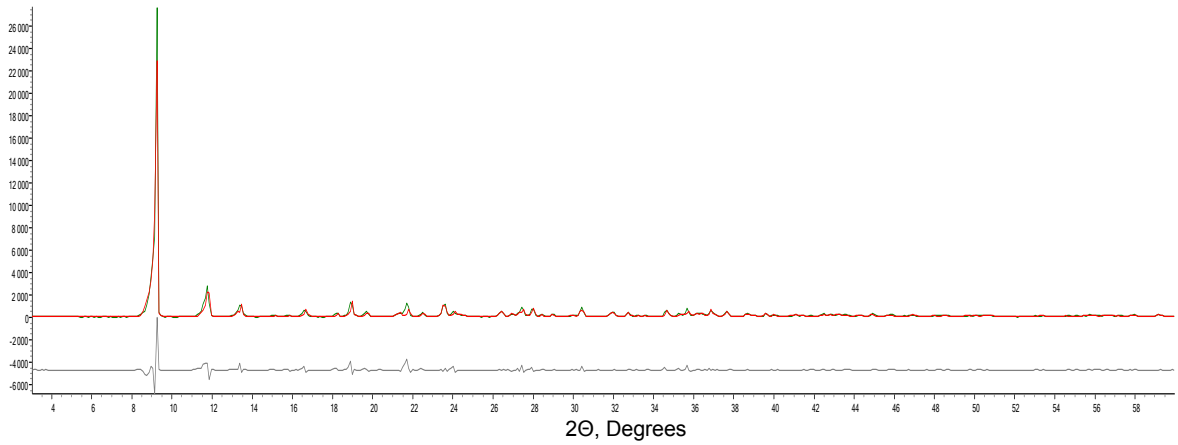

Figure S1. The results of Rietveld refinement for the polycrystalline product obtained by interaction of platinum NAS with $(Me_4N)NO_3$, showing experimental (green line) and calculated for the structure of **1** (red line) powder patterns and difference line (gray line below). Refined parameters: space group $P2_1/c$, a = 7.7874 Å, b = 15.1054 Å, c = 13.1794 Å, α = 90.00°, β = 104.60°, γ = 90.00°, R_{wp} = 24.5%.

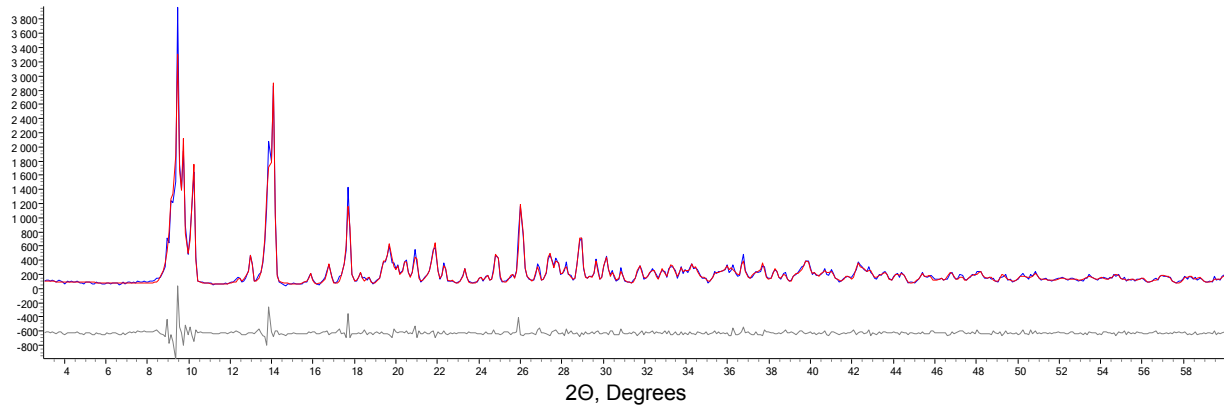

Figure S2. The results of Rietveld refinement for the polycrystalline product obtained by interaction of platinum NAS with $(Et_4N)NO_3$, showing experimental (blue line) and calculated for the structure of **2** (red line) powder patterns and difference line (gray line below). Refined parameters: space group P-1, a = 9.5083 Å, b = 10.0840 Å, c = 10.7494 Å, α = 114.21°, β = 94.75°, γ = 92.19°, R_{wp} = 10.9%.

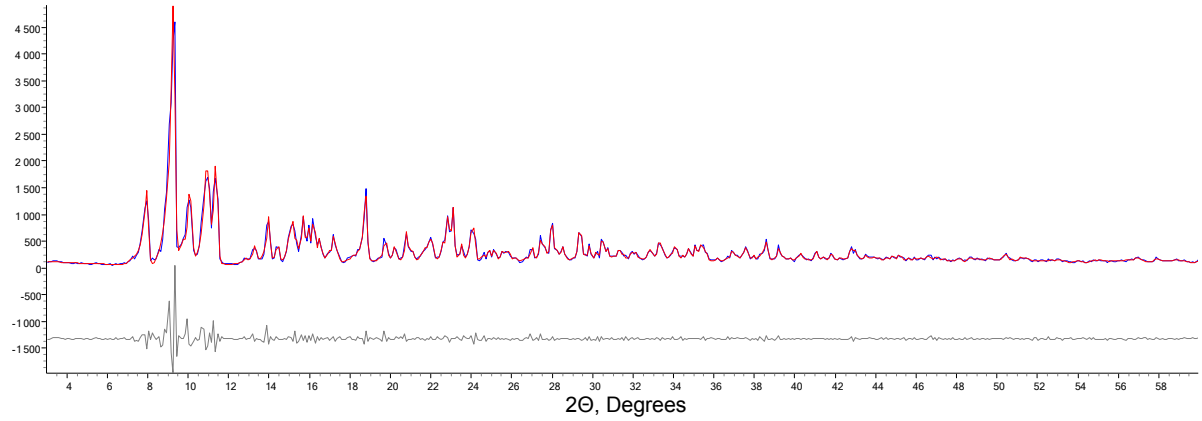

Figure S3. The results of Rietveld refinement for the polycrystalline product obtained by interaction of platinum NAS with $(n\text{-}Pr_4N)NO_3$, showing experimental (blue line) and calculated for the mixture of structures **3a** + **3b** (red line) powder patterns and difference line (gray line below). Refined parameters: (**3a**) space group P-1, a = 9.7710 Å, b = 11.0413 Å, c = 11.6146 Å, α = 116.06°, β = 102.35°, γ = 104.12°; (**3b**) space group $C2/c$, a = 18.0551 Å, b = 19.1710 Å, c = 15.0176 Å, α = 90.00°, β = 116.98°, γ = 90.00°. R_{wp} = 13.7%.

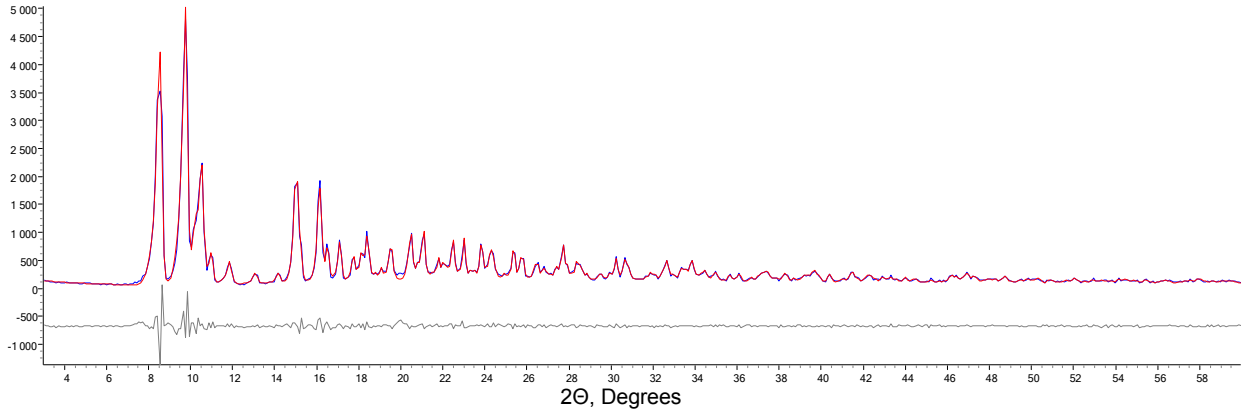

Figure S4. The results of Rietveld refinement for the polycrystalline product obtained by interaction of platinum NAS with (n-Bu_4N)NO_3, showing experimental (blue line) and calculated for the structure of **4** (red line) powder patterns and difference line (gray line below). Refined parameters: space group $P2_1/n$, a = 11.0146 Å, b = 16.1627 Å, c = 13.5735 Å, α = 90.00°, β = 91.61°, γ = 90.00°, R_{wp} = 9.1%.

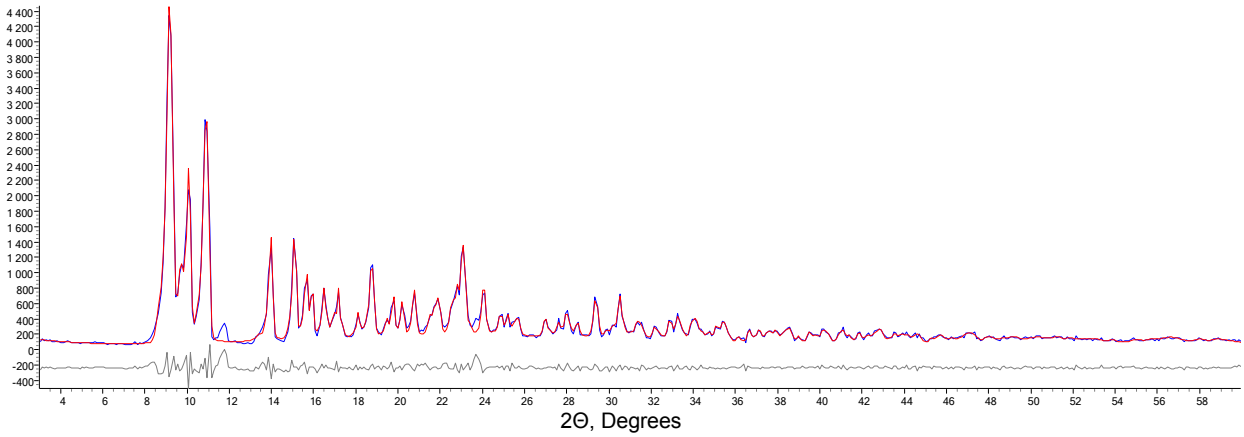

Figure S5. The results of Rietveld refinement for the polycrystalline sample of **3a** obtained by interaction metathesis reaction, showing experimental (blue line) and calculated for the structure of **3a** (red line) powder patterns and difference line (gray line below). Refined parameters: space group P-1, a = 9.7563 Å, b = 11.0275 Å, c = 11.6076 Å, α = 116.03°, β = 102.30°, γ = 104.27°, R_{wp} = 10.7%.

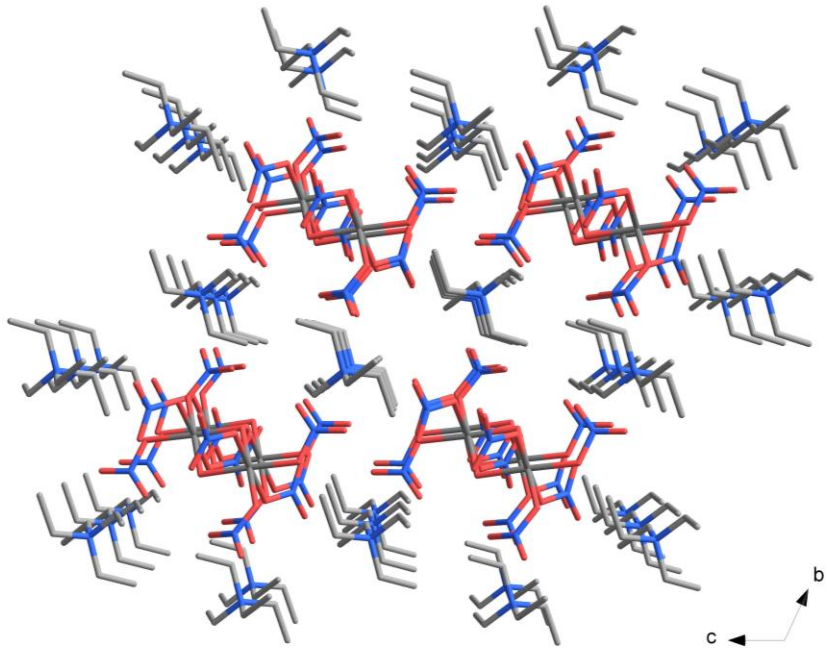

A

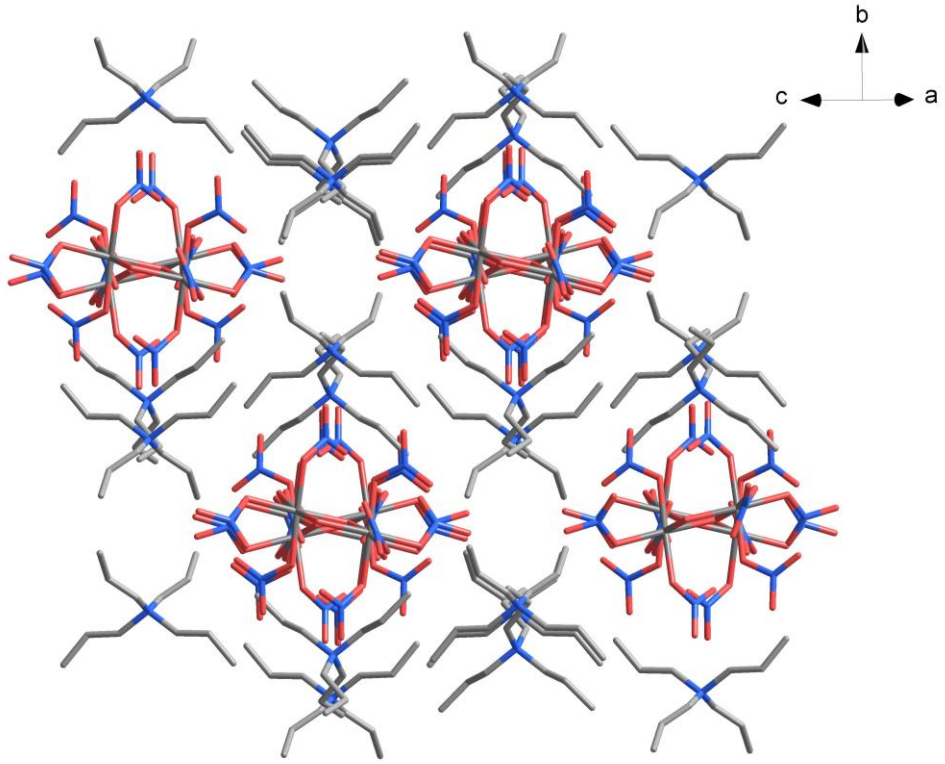

B

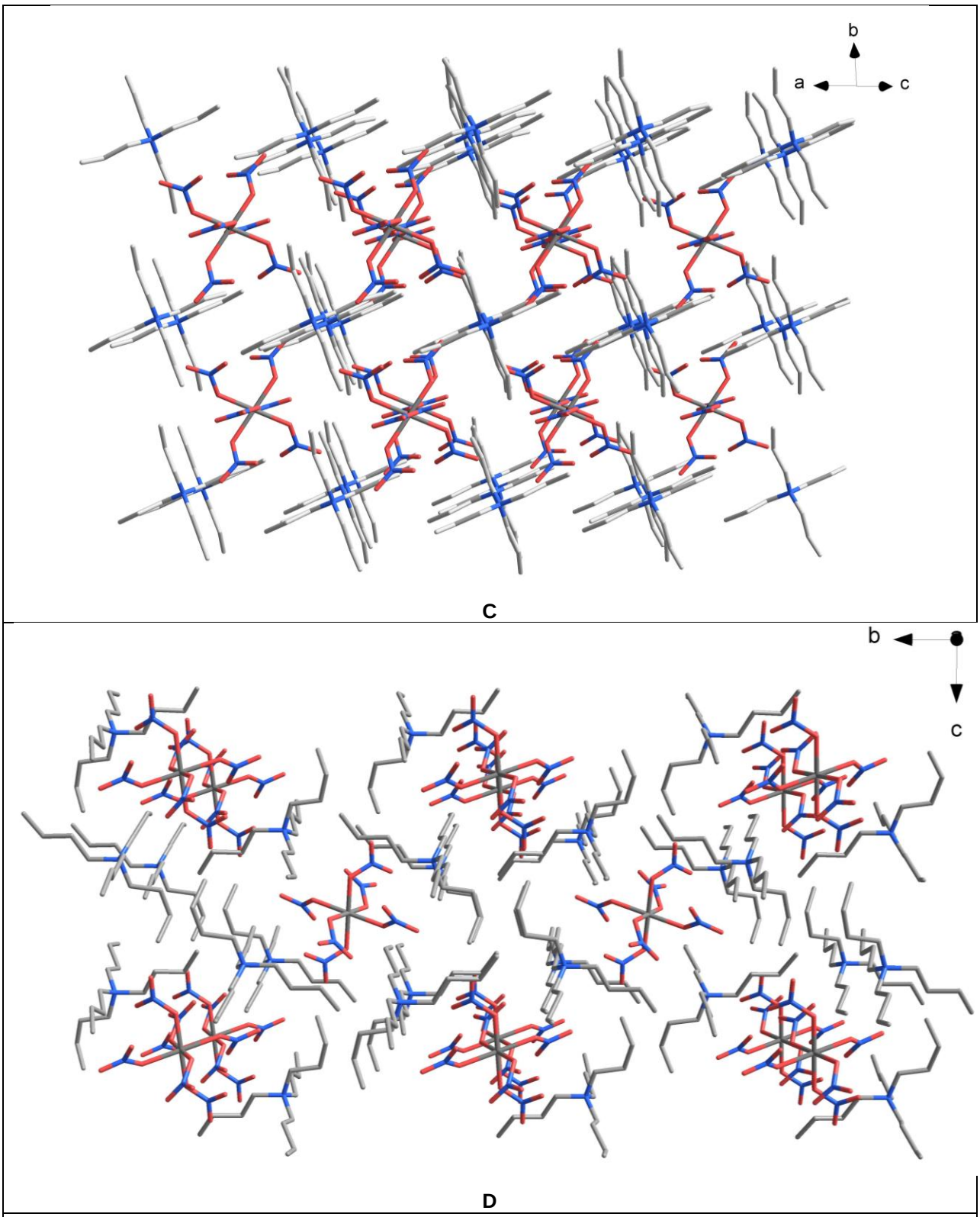

Figure S6. Packing diagrams for the structures of salts 2 (A), 3b (B) 3a (C) and 4 (D). Hydrogen atoms omitted for the sake of clarity.

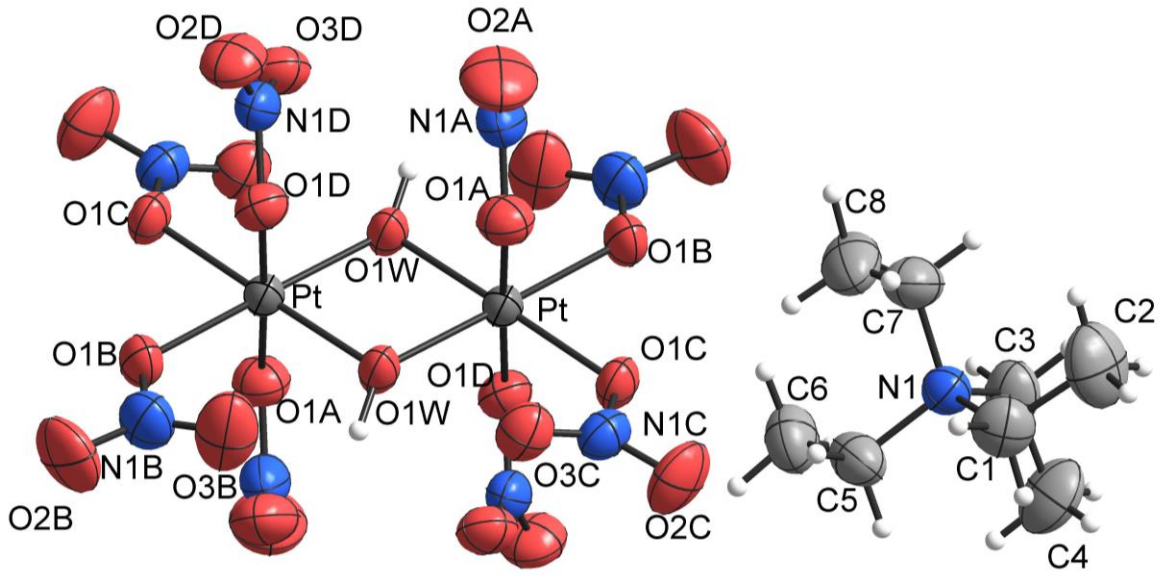

Figure S7. ORTEP view of the molecules in the structure of **2** with atom labelling scheme. Thermal ellipsoids are drawn at the 50% probability level.

Table S2. Selected bonds and angles for the structure of **2**.

Pt-O(1A)	1.999(3)	N(1)-C(7)	1.512(5)	O(2A)-N(1A)-O(3A)	127.4(5)
Pt-O(1C)	2.001(2)	C(1)-C(2)	1.529(8)	O(2A)-N(1A)-O(1A)	114.3(5)
Pt-O(1D)	2.006(3)	C(3)-C(4)	1.517(8)	O(3A)-N(1A)-O(1A)	118.3(4)
Pt-O(1B)	2.007(3)	C(5)-C(6)	1.516(7)	O(2B)-N(1B)-O(3B)	125.9(4)
Pt-O(1W)	2.018(2)	C(7)-C(8)	1.526(8)	O(2B)-N(1B)-O(1B)	114.6(4)
Pt-O(1W)#1	2.029(3)			O(3B)-N(1B)-O(1B)	119.4(4)
		O(1C)-Pt-O(1B)	75.04(11)	O(3C)-N(1C)-O(2C)	127.4(4)
O(1A)-N(1A)	1.334(5)	O(1A)-Pt-O(1C)	88.03(12)	O(3C)-N(1C)-O(1C)	119.8(3)
N(1A)-O(2A)	1.192(6)	O(1A)-Pt-O(1D)	177.74(11)	O(2C)-N(1C)-O(1C)	112.8(4)
N(1A)-O(3A)	1.223(6)	O(1C)-Pt-O(1D)	89.76(11)	O(2D)-N(1D)-O(3D)	127.1(4)
O(1B)-N(1B)	1.326(5)	O(1A)-Pt-O(1B)	92.17(13)	O(2D)-N(1D)-O(1D)	113.6(3)
N(1B)-O(2B)	1.200(5)	N(1)-C(7)	1.512(5)	O(3D)-N(1D)-O(1D)	119.3(3)
N(1B)-O(3B)	1.208(6)	O(1D)-Pt-O(1B)	86.80(12)		
O(1C)-N(1C)	1.358(4)	O(1A)-Pt-O(1W)	94.48(13)	C(5)-N(1)-C(3)	111.3(3)
N(1C)-O(3C)	1.195(5)	O(1C)-Pt-O(1W)	177.47(11)	C(5)-N(1)-C(1)	106.7(3)
N(1C)-O(2C)	1.204(5)	O(1D)-Pt-O(1W)	87.72(12)	C(3)-N(1)-C(1)	110.4(3)
O(1D)-N(1D)	1.359(4)	O(1B)-Pt-O(1W)	104.51(11)	C(5)-N(1)-C(7)	110.9(3)
N(1D)-O(2D)	1.203(5)	O(1A)-Pt-O(1W)#1	85.74(12)	C(3)-N(1)-C(7)	106.2(3)
N(1D)-O(3D)	1.212(5)	O(1C)-Pt-O(1W)#1	104.65(11)	C(1)-N(1)-C(7)	111.4(4)
		O(1D)-Pt-O(1W)#1	95.28(12)	N(1)-C(1)-C(2)	115.0(4)
N(1)-C(5)	1.505(5)	O(1B)-Pt-O(1W)#1	177.90(11)	N(1)-C(3)-C(4)	114.7(4)
N(1)-C(3)	1.511(5)	O(1W)-Pt-O(1W)#1	75.89(11)	N(1)-C(5)-C(6)	115.6(4)
N(1)-C(1)	1.511(5)	Pt-O(1W)-Pt#1	104.11(11)	N(1)-C(7)-C(8)	113.9(4)

#1 -x+1,-y+1,-z+1

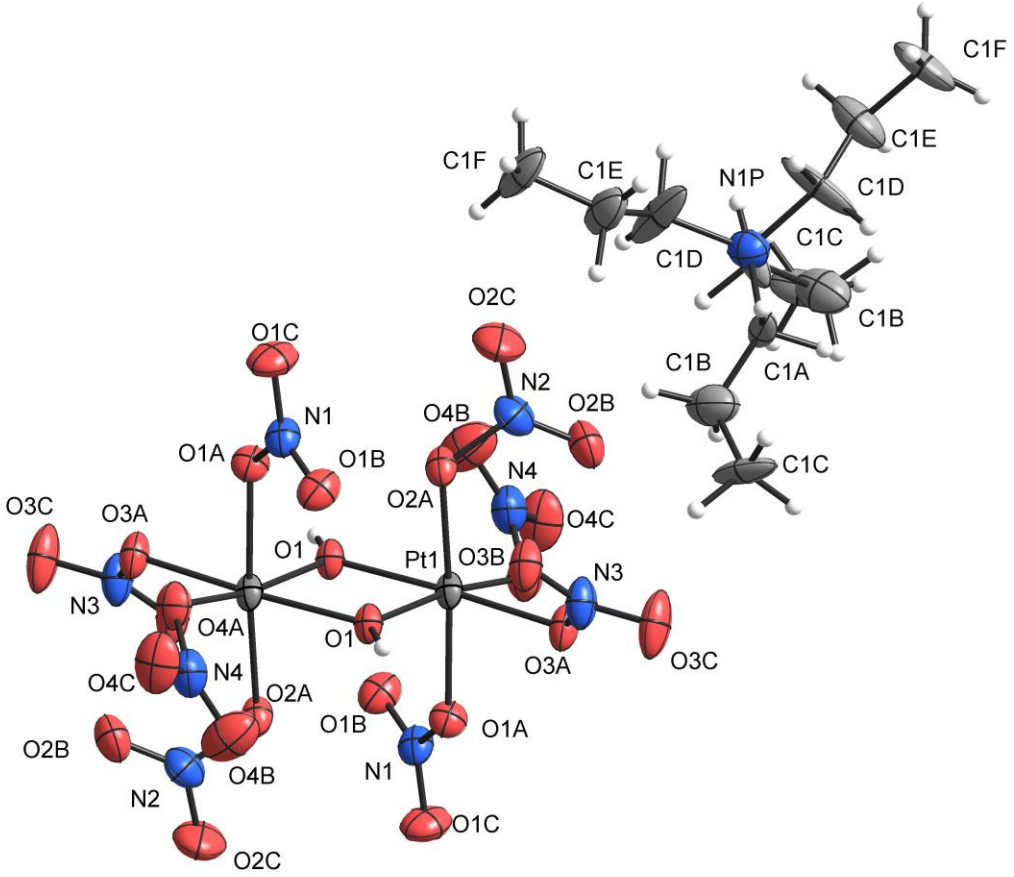

Figure S8. ORTEP view of the molecules in the structure of **3b** with atom labelling scheme. Thermal ellipsoids are drawn at the 50% probability level.

Table S3. Selected bonds and angles for the structure of (**3b**)

Pt(1)-O(4A)	1.986(3)	C(2A2)-C(2B2)	1.511(11)	O(4C)-N(4)-O(4A)	112.6(4)
Pt(1)-O(2A)	1.990(3)	C(2D1)-C(2E1)	1.495(10)	N(4)-O(4A)-Pt(1)	118.3(2)
Pt(1)-O(3A)	1.996(3)	C(2E1)-C(2F)	1.548(9)	C(1D)-N(1P)-C(1D)#2	108.0(15)
Pt(1)-O(1A)	2.003(3)	C(2F)-C(2E2)	1.431(11)	C(1D)-N(1P)-C(1A)#2	108.7(5)
Pt(1)-O(1)	2.023(2)	C(2D2)-C(2E2)	1.522(11)	C(1D)-N(1P)-C(1A)	107.7(7)
Pt(1)-O(1)#1	2.024(3)			C(1A)#2-N(1P)-C(1A)	115.8(9)
		O(4A)-Pt(1)-O(2A)	103.35(14)	C(1B)-C(1A)-N(1P)	122.4(10)
N(1)-O(1C)	1.217(5)	O(4A)-Pt(1)-O(3A)	81.97(13)	C(1A)-C(1B)-C(1C)	102.8(12)
N(1)-O(1B)	1.224(5)	O(2A)-Pt(1)-O(3A)	100.31(12)	C(1E)-C(1D)-N(1P)	139.8(12)
N(1)-O(1A)	1.340(4)	O(4A)-Pt(1)-O(1A)	84.22(13)	C(1D)-C(1E)-C(1F)	132.6(14)
N(2)-O(2B)	1.214(5)	O(2A)-Pt(1)-O(1A)	172.43(13)	C(2A1)#3-N(2P)-C(2A1)	142.9(6)
N(2)-O(2C)	1.216(5)	O(3A)-Pt(1)-O(1A)	80.23(12)	C(2A1)#3-N(2P)-C(2D1)	96.9(4)
N(2)-O(2A)	1.360(5)	O(4A)-Pt(1)-O(1)	99.75(11)	C(2A1)-N(2P)-C(2D1)	112.0(4)
N(3)-O(3B)	1.205(5)	O(2A)-Pt(1)-O(1)	81.66(11)	C(2A1)#3-N(2P)-C(2D1)#3	112.0(4)
N(3)-O(3C)	1.227(5)	O(3A)-Pt(1)-O(1)	177.06(13)	C(2A1)-N(2P)-C(2D1)#3	96.9(4)
N(3)-O(3A)	1.368(4)	O(1A)-Pt(1)-O(1)	97.53(11)	C(2D1)-N(2P)-C(2D1)#3	78.1(5)
N(4)-O(4B)	1.192(5)	O(4A)-Pt(1)-O(1)#1	170.35(12)	C(2A1)#3-N(2P)-C(2A2)	110.0(5)
N(4)-O(4C)	1.226(6)	O(2A)-Pt(1)-O(1)#1	86.04(13)	C(2A1)-N(2P)-C(2A2)	34.7(4)
N(4)-O(4A)	1.365(6)	O(3A)-Pt(1)-O(1)#1	98.72(12)	C(2D1)-N(2P)-C(2A2)	144.3(4)
N(1P)-C(1D)	1.477(9)	O(1A)-Pt(1)-O(1)#1	86.41(12)	C(2D1)#3-N(2P)-C(2A2)	111.0(3)
N(1P)-C(1A)	1.489(7)	O(1)-Pt(1)-O(1)#1	79.19(12)	C(2A2)-N(2P)-C(2A2)#3	82.2(6)
C(1A)-C(1B)	1.365(14)			C(2A1)-N(2P)-C(2D2)#3	111.4(4)
C(1B)-C(1C)	1.678(19)	Pt(1)-O(1)-Pt(1)#1	100.81(12)	C(2D1)-N(2P)-C(2D2)#3	106.5(4)
C(1D)-C(1E)	1.241(14)	O(1C)-N(1)-O(1B)	125.0(4)	C(2D1)#3-N(2P)-C(2D2)#3	40.7(4)
C(1E)-C(1F)	1.393(13)	O(1C)-N(1)-O(1A)	114.0(4)	C(2A2)-N(2P)-C(2D2)#3	101.0(4)
N(2P)-C(2A1)	1.472(8)	O(1B)-N(1)-O(1A)	120.9(3)	C(2A1)-N(2P)-C(2D2)	80.2(4)
N(2P)-C(2D1)	1.505(7)	N(1)-O(1A)-Pt(1)	120.0(3)	C(2A2)-N(2P)-C(2D2)	105.6(4)
N(2P)-C(2A2)	1.543(7)	O(2B)-N(2)-O(2C)	125.8(4)	C(2D2)#3-N(2P)-C(2D2)	144.4(6)
N(2P)-C(2D2)	1.583(8)	O(2B)-N(2)-O(2A)	120.5(4)	N(2P)-C(2A1)-C(2B1)	116.6(7)
C(2A1)-C(2B1)	1.520(10)	O(2C)-N(2)-O(2A)	113.6(4)	C(2A1)-C(2B1)-C(2C)	112.3(8)
C(2B1)-C(2C)	1.524(12)	N(2)-O(2A)-Pt(1)	120.5(2)	C(2B2)-C(2C)-C(2B1)	45.3(5)
C(2C)-C(2B2)	1.471(9)	O(3B)-N(3)-O(3C)	127.0(4)	C(2B2)-C(2A2)-N(2P)	116.3(5)
		O(3B)-N(3)-O(3A)	120.3(3)	C(2C)-C(2B2)-C(2A2)	111.6(7)
		O(3C)-N(3)-O(3A)	112.7(4)	C(2E1)-C(2D1)-N(2P)	115.0(5)
		N(3)-O(3A)-Pt(1)	118.0(2)	C(2D1)-C(2E1)-C(2F)	111.4(6)
		O(4B)-N(4)-O(4C)	127.4(5)	C(2E2)-C(2D2)-N(2P)	113.7(6)
		O(4B)-N(4)-O(4A)	120.0(5)	C(2F)-C(2E2)-C(2D2)	112.0(7)

#1 -x+1/2,-y+1/2,-z+1 #2 -x+1,y,-z+1/2 #3 -x,y,-z+3/2

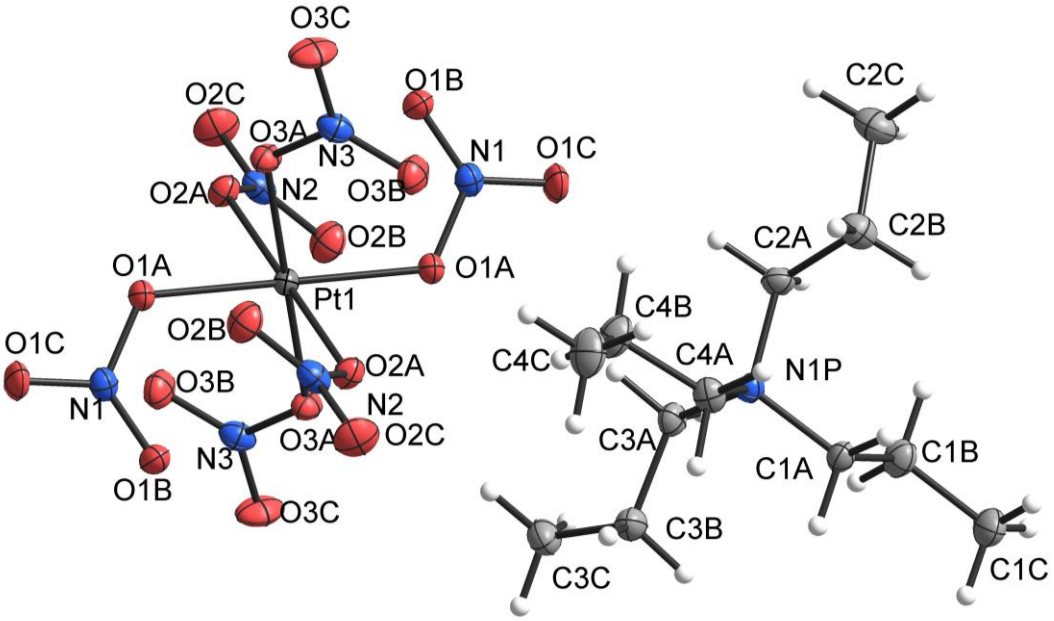

Figure S9. ORTEP view of the molecules in the structure of **3a** with atom labelling scheme. Thermal ellipsoids are drawn at the 50% probability level.

Table S4. Selected bonds and angles for the structure of **3a**.

Pt1—O2A^{i}	2.0064(12)	C3A—C3B	1.510(3)	O1B—N1—O1A	120.28(15)
Pt1—O2A	2.0065(12)	C3B—C3C	1.526(3)	O1C—N1—O1A	113.99(16)
Pt1—O1A^{i}	2.0094(12)	C4A—C4B	1.514(3)	O2C—N2—O2B	126.74(17)
Pt1—O1A	2.0094(12)	C4B—C4C	1.525(3)	O2C—N2—O2A	113.68(16)
Pt1—O3A	2.0098(13)			O2B—N2—O2A	119.58(15)
Pt1—O3A^{i}	2.0099(13)	O2A^{i}—Pt1—O2A	180.000	O3C—N3—O3B	125.75(16)
O1A—N1	1.336(2)	O2A^{i}—Pt1—O1A^{i}	79.69(5)	O3C—N3—O3A	114.41(15)
O1B—N1	1.215(2)	O2A—Pt1—O1A^{i}	100.32(5)	O3B—N3—O3A	119.84(16)
O1C—N1	1.221(2)	O2A^{i}—Pt1—O1A	100.31(5)		
O2A—N2	1.350(2)	O2A—Pt1—O1A	79.68(5)	C2A—N1P—C1A	111.51(15)
O2B—N2	1.219(2)	O1A^{i}—Pt1—O1A	180.000	C2A—N1P—C4A	111.52(15)
O2C—N2	1.213(2)	O2A^{i}—Pt1—O3A	100.54(5)	C1A—N1P—C4A	105.41(14)
O3A—N3	1.3372(19)	O2A—Pt1—O3A	79.46(5)	C2A—N1P—C3A	105.60(13)
O3B—N3	1.221(2)	O1A^{i}—Pt1—O3A	101.21(5)	C1A—N1P—C3A	111.60(15)
O3C—N3	1.217(2)	O1A—Pt1—O3A	78.79(5)	C4A—N1P—C3A	111.33(14)
		O2A^{i}—Pt1—O3A^{i}	79.46(5)	C1B—C1A—N1P	116.11(15)
N1P—C2A	1.518(2)	O2A—Pt1—O3A^{i}	100.54(5)	C1A—C1B—C1C	109.61(17)
N1P—C1A	1.521(2)	O1A^{i}—Pt1—O3A^{i}	78.79(5)	C2B—C2A—N1P	117.42(15)
N1P—C4A	1.521(2)	O1A—Pt1—O3A^{i}	101.21(5)	C2A—C2B—C2C	108.72(17)
N1P—C3A	1.526(2)	O3A—Pt1—O3A^{i}	180.000	C3B—C3A—N1P	116.65(15)
C1A—C1B	1.510(3)	N1—O1A—Pt1	120.71(11)	C3A—C3B—C3C	109.22(16)
C1B—C1C	1.524(3)	N2—O2A—Pt1	120.66(11)	C4B—C4A—N1P	116.70(15)
C2A—C2B	1.513(3)	N3—O3A—Pt1	120.99(11)	C4A—C4B—C4C	108.33(17)
C2B—C2C	1.524(3)	O1B—N1—O1C	125.74(17)		

(i) 1-x, 1-y, -z.

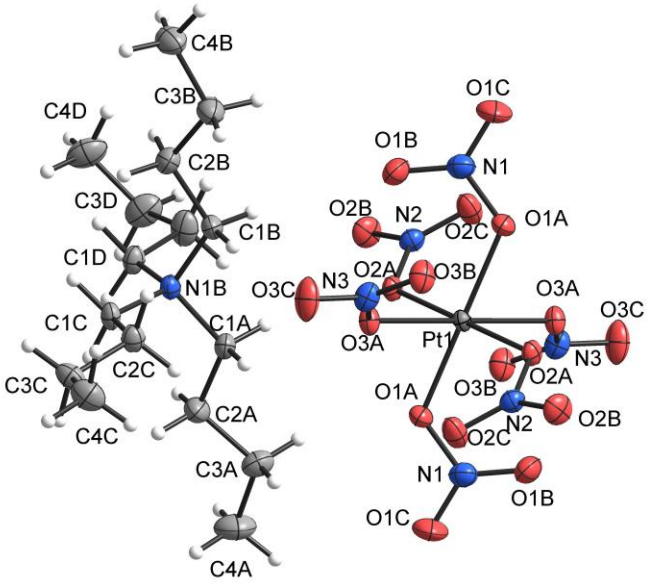

Figure S10. ORTEP view of the molecules in the structure of **4** with atom labelling scheme. Thermal ellipsoids are drawn at the 50% probability level.

Table S5. Selected bonds and angles for the structure of **4**.

Pt(1)-O(1A)	2.0074(16)	C(1C)-C(2C)	1.519(3)	O(3C)-N(3)-O(3B)	126.6(2)
Pt(1)-O(2A)	2.0088(15)	C(2C)-C(3C)	1.523(3)	O(3C)-N(3)-O(3A)	113.51(19)
Pt(1)-O(3A)	2.0130(15)	C(3C)-C(4C)	1.521(4)	O(3B)-N(3)-O(3A)	119.92(19)
N(1)-O(1B)	1.217(3)	C(1D)-C(2D)	1.523(3)	N(3)-O(3A)-Pt(1)	121.11(13)
N(1)-O(1C)	1.217(3)	C(2D)-C(3D)	1.532(4)	C(1D)-N(1B)-C(1B)	111.32(17)
N(1)-O(1A)	1.345(3)	C(3D)-C(4D)	1.512(4)	C(1D)-N(1B)-C(1C)	106.28(16)
N(2)-O(2C)	1.214(3)			C(1B)-N(1B)-C(1C)	111.00(17)
N(2)-O(2B)	1.222(2)			C(1D)-N(1B)-C(1A)	111.32(17)
N(2)-O(2A)	1.356(2)	O(1A)-Pt(1)-O(2A)#1	80.17(6)	C(1B)-N(1B)-C(1A)	106.54(16)
N(3)-O(3C)	1.218(3)	O(1A)-Pt(1)-O(2A)	99.83(6)	C(1C)-N(1B)-C(1A)	110.45(17)
N(3)-O(3B)	1.218(3)	O(1A)-Pt(1)-O(3A)#1	79.34(7)	C(2A)-C(1A)-N(1B)	116.28(18)
N(3)-O(3A)	1.342(2)	O(2A)-Pt(1)-O(3A)#1	100.71(6)	C(1A)-C(2A)-C(3A)	109.8(2)
N(1B)-C(1D)	1.519(3)	O(1A)-Pt(1)-O(3A)	100.66(7)	C(2A)-C(3A)-C(4A)	112.9(2)
N(1B)-C(1B)	1.521(3)	O(2A)-Pt(1)-O(3A)	79.29(6)	C(2B)-C(1B)-N(1B)	115.32(18)
N(1B)-C(1C)	1.523(3)	O(1B)-N(1)-O(1C)	126.3(2)	C(1B)-C(2B)-C(3B)	110.7(2)
N(1B)-C(1A)	1.526(3)	O(1B)-N(1)-O(1A)	120.1(2)	C(4B)-C(3B)-C(2B)	112.0(2)
C(1A)-C(2A)	1.515(3)	O(1C)-N(1)-O(1A)	113.6(2)	C(2C)-C(1C)-N(1B)	116.00(18)
C(2A)-C(3A)	1.521(4)	N(1)-O(1A)-Pt(1)	121.20(14)	C(1C)-C(2C)-C(3C)	109.58(19)
C(3A)-C(4A)	1.526(4)	O(2C)-N(2)-O(2B)	126.2(2)	C(4C)-C(3C)-C(2C)	112.1(2)
C(1B)-C(2B)	1.521(3)	O(2C)-N(2)-O(2A)	120.38(18)	N(1B)-C(1D)-C(2D)	114.88(19)
C(2B)-C(3B)	1.526(4)	O(2B)-N(2)-O(2A)	113.46(18)	C(1D)-C(2D)-C(3D)	110.8(2)
C(3B)-C(4B)	1.524(4)	N(2)-O(2A)-Pt(1)	121.14(12)	C(4D)-C(3D)-C(2D)	114.1(3)

#1 -x+1,-y+1,-z+2

Table S6. Cartesian coordinates (Angström) for DFT calculated structure of $[Pt(NO_3)_6]^{2-}$ anion. .

Atom type	x	y	z	Atom type	x	y	z
Pt	0.000121	0.000322	-0.000017	N	2.867998	0.050595	-1.034587
N	-2.867726	-0.051895	1.034728	O	1.523048	0.026858	-1.393501
O	-1.522776	-0.026287	1.393530	O	3.668902	0.072810	-2.018350
O	-3.668527	-0.073612	2.018583	O	3.188058	0.047730	0.196157
O	-3.187919	-0.051205	-0.195982	N	-1.390203	-2.508652	-1.034680
N	1.390620	2.509156	1.034675	O	-0.737302	-1.332331	-1.393709
O	0.737879	1.332749	1.393703	O	-1.770462	-3.213886	-2.018342
O	1.770967	3.214342	2.018339	O	-1.554900	-2.783531	0.195881
O	1.554987	2.784194	-0.195899	N	1.480000	-2.456092	1.035029
N	-1.480350	2.456377	-1.035123	O	0.782109	-1.306353	1.395233
O	-0.781960	1.306944	-1.395302	O	1.898598	-3.140696	2.017678
O	-1.900247	3.140170	-2.017785	O	1.640263	-2.731513	-0.196057
O	-1.642194	2.730929	0.195951				

Table S7. Cartesian coordinates (Angström) for DFT calculated structure of $[Pt_2(NO_3)_8(OH)_2]^{2-}$ anion ("symmetric" conformation)

Atom type	x	y	z	Atom type	x	y	z
Pt	1.637636	-0.000481	-0.000313	Pt	-1.636062	0.000405	0.000133
O	0.000417	-0.912036	0.842127	O	0.000739	0.911454	-0.843038
H	-0.001109	-1.061977	1.816754	H	-0.000540	1.060165	-1.817814
O	1.637248	-1.382756	-1.514320	O	-1.633613	1.345633	1.546909
N	1.819596	-2.754945	-1.248141	N	-1.820375	2.723257	1.317745
O	1.882097	-3.470846	-2.290740	O	-1.887964	3.410832	2.378868
O	1.894073	-3.157794	-0.048680	O	-1.893649	3.157125	0.129006
O	3.239798	-0.859896	0.940664	O	-3.238300	0.874968	-0.926936
N	3.048278	-1.465990	2.190697	N	-3.049842	1.503078	-2.166473
O	4.086394	-1.990069	2.679149	O	-4.089628	2.035135	-2.642918
O	1.893470	-1.438307	2.726680	O	-1.896501	1.485938	-2.705920
O	3.240115	0.858733	-0.940883	O	-3.238141	-0.873429	0.928143
N	3.048904	1.465174	-2.190781	N	-3.049295	-1.501759	2.167517
O	4.086900	1.990460	-2.678268	O	-4.088994	-2.033745	2.644241
O	1.894570	1.436367	-2.727657	O	-1.895852	-1.484706	2.706714
O	1.638793	1.381839	1.513575	O	-1.636226	-1.344809	-1.546590
N	1.821457	2.754019	1.247090	N	-1.823174	-2.722409	-1.316998
O	1.886101	3.469760	2.289654	O	-1.893344	-3.409917	-2.377964
O	1.894205	3.156939	0.047601	O	-1.893957	-3.156282	-0.128112

Table S8. Cartesian coordinates (Angström) for DFT calculated structure of $[Pt_2(NO_3)_8(OH)_2]^{2-}$ anion ("angled" conformation).

Atom type	x	y	z	Atom type	x	y	z
Pt	-1.583175	-0.289729	-0.247426	Pt	1.583672	0.287715	0.247259
O	-0.015580	-0.765189	1.012728	O	0.016741	0.761022	-1.014426
O	-3.154002	-1.424740	0.412152	O	3.154520	1.422361	-0.412811
O	-2.186436	2.353474	-1.706556	O	2.179343	-2.348119	1.730647
O	-1.199076	-1.702610	-1.695219	O	1.198710	1.701747	1.693738
O	-1.824497	1.188429	1.154576	O	1.828695	-1.184656	-1.160537
O	-3.024339	0.209472	-1.619944	O	3.022166	-0.206054	1.625232
O	-4.049710	1.585107	0.663631	O	4.053567	-1.583877	-0.668869
O	-2.023935	-2.076519	2.320779	O	2.025722	2.072620	-2.322950
O	-4.138218	-2.772524	1.906259	O	4.141169	2.765625	-1.909535
O	-0.526367	-3.234359	-0.105406	O	0.519096	3.231185	0.105353
O	-0.582146	-3.769077	-2.303354	O	0.578456	3.766924	2.303167
O	-3.016603	2.624010	2.390231	O	3.025756	-2.605130	-2.408853
N	-3.066755	1.522749	-2.106266	N	3.060930	-1.515130	2.123016
N	-3.084624	-2.133658	1.628912	N	3.086526	2.129046	-1.631153
N	-3.053971	1.827971	1.408033	N	3.058706	-1.822040	-1.416275
N	-0.745841	-2.976407	-1.336740	N	0.732019	2.971130	1.337378
O	-4.000716	1.750465	-2.921922	O	4.003895	-1.742645	2.928093
H	0.136259	-1.739766	1.102692	H	-0.133708	1.735665	-1.107612

Table S9. Selected major DFT calculated IR vibrational frequencies for $[Pt(NO_3)_6]^{2-}$ anion.

Assignment	Wavenumber, cm^{-1}
$v_5(NO_3)$	1420
$v_1(O\text{-}NO_2)$	1157
$v_2(NO_3)$	869
$v(Pt\text{-}ONO_2)$	312

Table S10. Selected major DFT calculated IR vibrational frequencies for $[Pt_2(NO_3)_8(OH)_2]^{2-}$ anion ("symmetric" conformation).

Assignment	Wavenumber, cm^{-1}
$v_5(NO_3)$	1440-1460
$v_1(O\text{-}NO_2)$	1160-1190,
$v_2(NO_3)$	840-900
δ(O-H)	674
$\delta(Pt(\mu\text{-}OH)_2Pt)_{ring}$	524
v(Pt-OH)	448
$v(Pt\text{-}ONO_2)$	340, 277

Table S11. Selected major DFT calculated IR vibrational frequencies for $[Pt_2(NO_3)_8(OH)_2]^{2-}$ anion ("angled" conformation).

Assignment	Wavenumber, cm^{-1}
$v_5(NO_3)$	1450-1460
$v_1(O\text{-}NO_2)$	1150-1200,
$v_2(NO_3)$	840-900
δ(O-H)	735
$\delta(Pt(\mu\text{-}OH)_2Pt)_{ring}$	524
v(Pt-OH)	465
$v(Pt\text{-}ONO_2)$	322, 332, 291

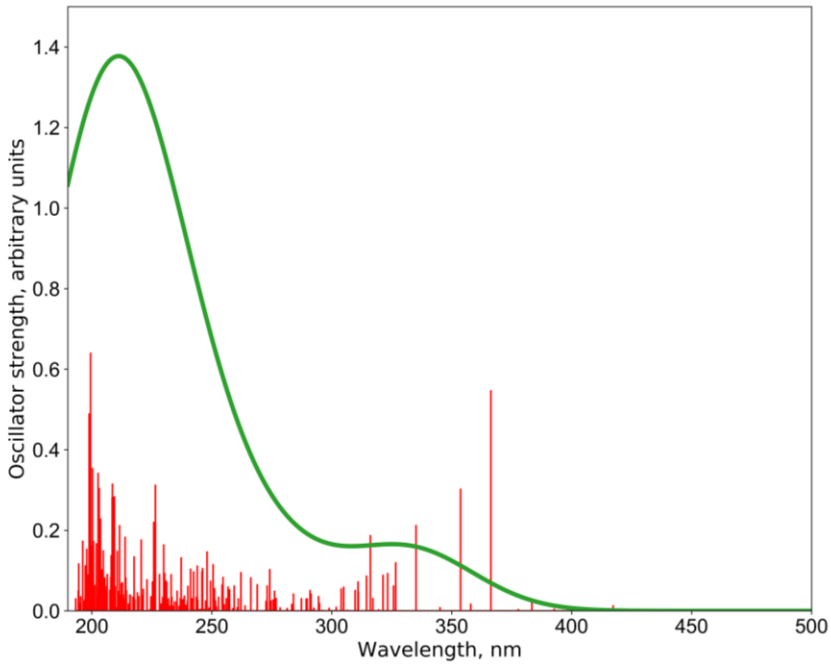

Figure S11. sTD-DFT (B3LYP, COSMO) calculated vertical transitions for $[Pt_2(OH)_2(NO_3)_8]^{2-}$ anion in "angled" conformation (red vertical lines, height corresponds to the oscillator strength) and corresponding predicted UV−vis absorption spectra (green line) computed with ADF-2017 software using "equal area gaussian" mode.

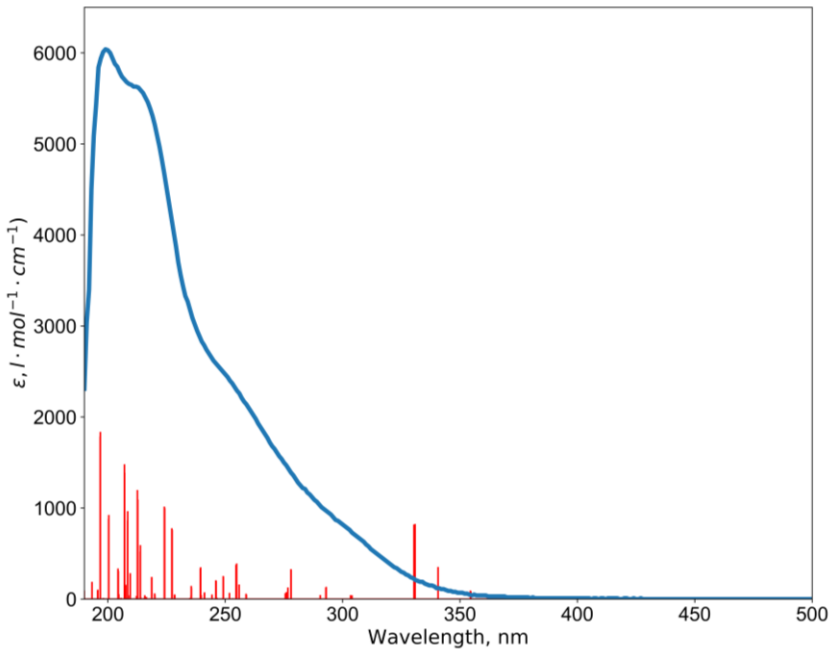

Figure S12. UV−vis absorption spectra of **4** (blue line) in acetone and sTD-DFT (B3LYP, COSMO) calculated vertical transitions for $[Pt(NO_3)_6]^{2-}$ anion (red vertical lines, height corresponds to the oscillator strength).

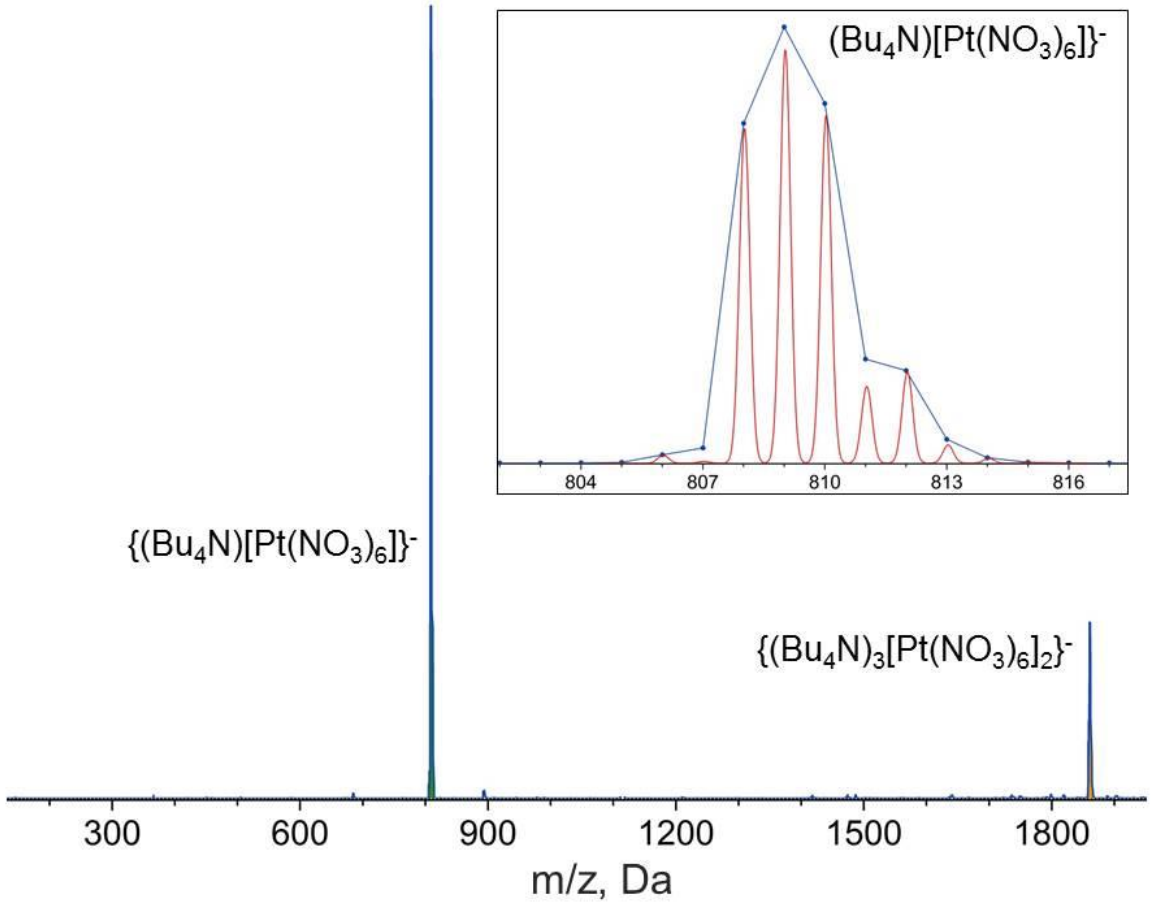

Figure S13. ESI-MS spectrum of salt **4** electrosprayed out of acetonitrile solution. Labels mark positions of the signals corresponding to the $\{(Bu_4N)[Pt(NO_3)_6]\}^-$ and $\{(Bu_4N)_3[Pt(NO_3)_6]_2\}^-$ anionic species. Inset shows the comparison between the experimental (blue line and dots) and the theoretical (red line) spectrum of $\{(Bu_4N)[Pt(NO_3)_6]\}^-$ anion.

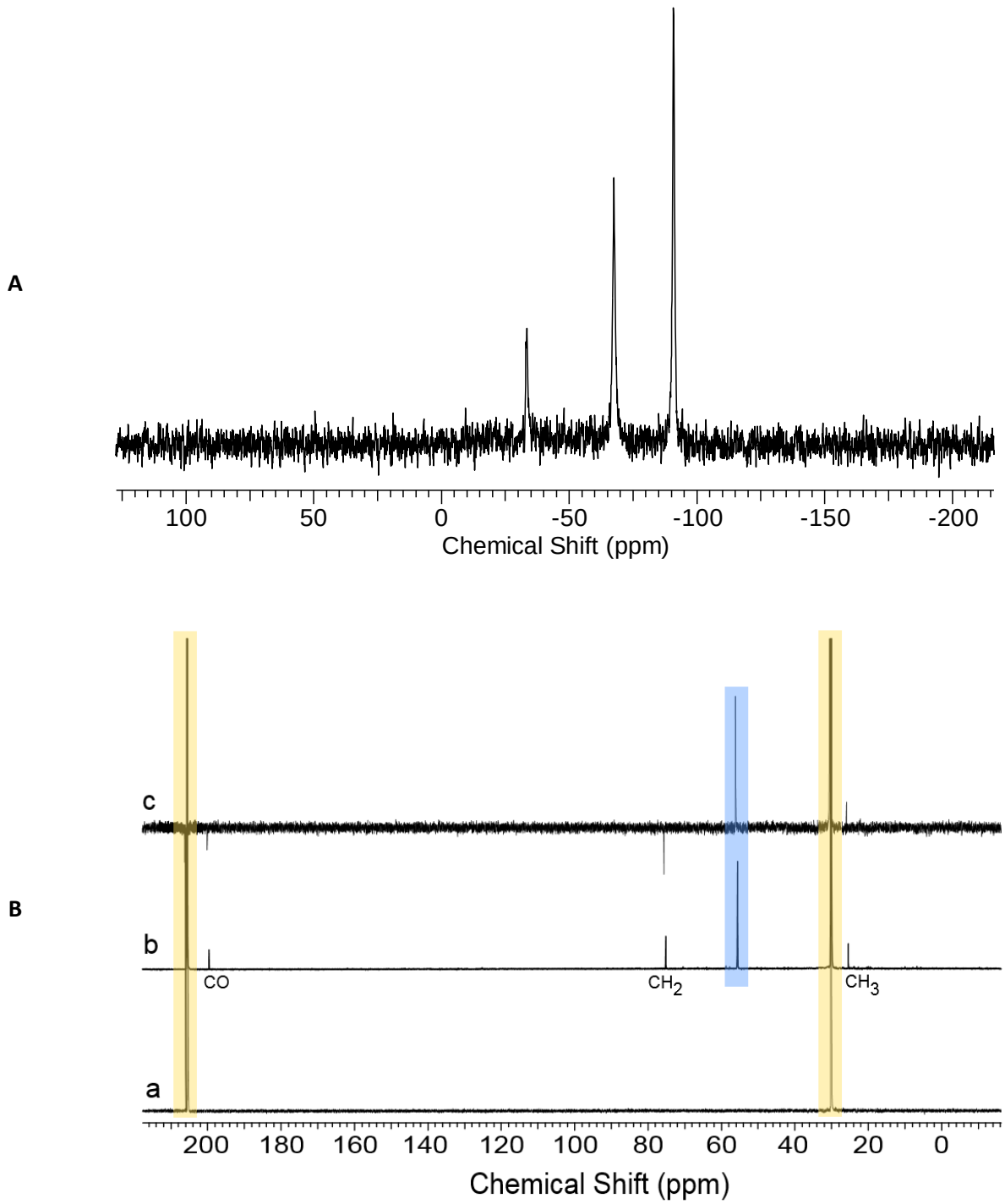

Figure S14. (A) ^{195}Pt NMR spectrum of the **1** acetone solution aged for 10 h at 20°C. (B) ^{13}C NMR spectra of acetone (a) and the aged acetone solution of **1** (b). The spectrum (c) depicts the SEFT-^{13}C NMR spectrum (signals of CH_3 and CH groups becomes positive while C and CH_2 negative) of the same solution. The signals of the solvent (acetone) are marked with yellow; the signal of $(CH_3)_4N^+$ cation is marked with blue. The signals ascribed to the product of interaction of acetone and $[Pt_2(OH)_2(NO_3)_8]^{2-}$ are labeled with a text.

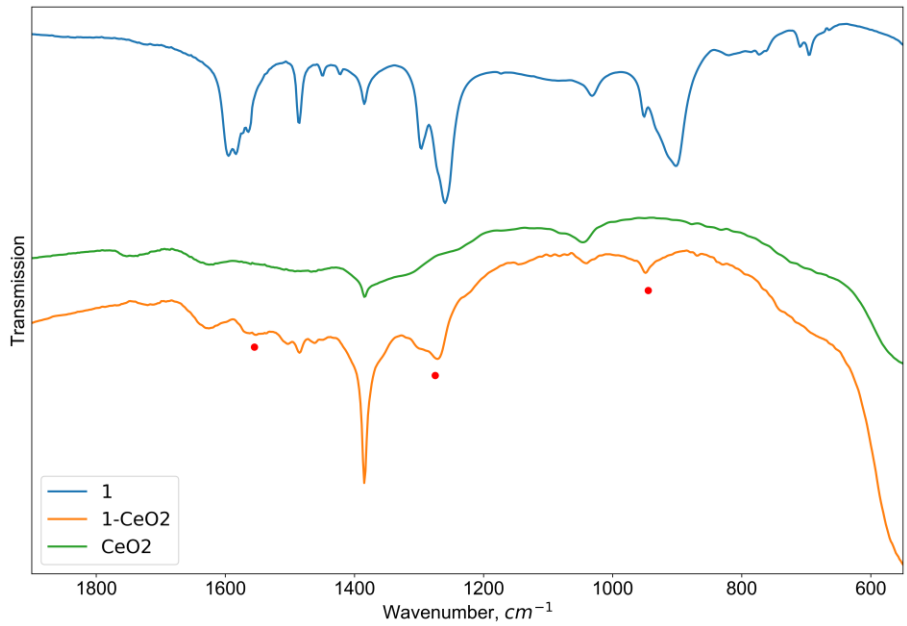

Figure S15. FT-IR spectra of the salt **1**, CeO_2 carrier and the **1**-CeO_2 material obtained by deposition of $[Pt_2(NO_3)_8(OH)_2]^{2-}$ on the surface of CeO_2. Signals attributed to the platinum nitrato complex are marked with red circles.

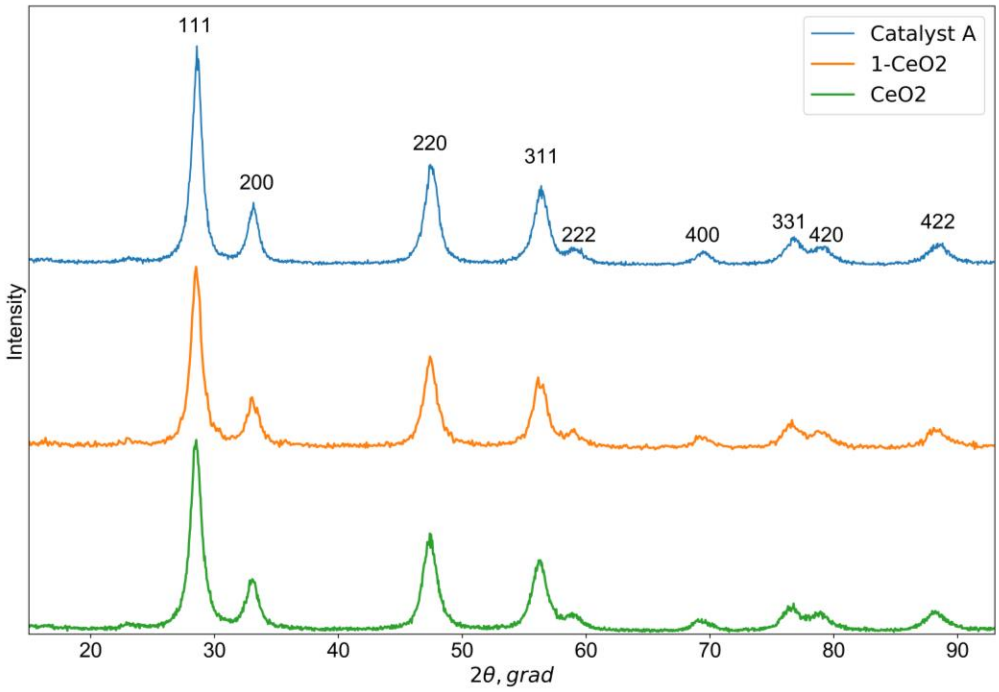

Figure S16. X-ray powder diffraction patterns of CeO_2, sample obtained by deposition of $[Pt_2(NO_3)_8(OH)_2]^{2-}$ on the surface of CeO_2 (**1**-CeO_2) and catalyst **A** after testing in the CO+O_2 reaction. The Miller *hkl* indices of CeO_2 fluorite structure are shown.

Table S12. Atomic percentages and speciation in the as-prepared product **1**-CeO_2 and catalyst **A** calculated from XPS data.

Sample	Atomic percentages and fraction of the species													
	Pt	Pt^0	Pt^{2+}	Pt^{4+}	**C**	CC, CH	O-C=O	**N**	**O**	O-Ce	O-II	O-III	**Ce**	**Ce^{3+}/Ce**
CeO_2	-	-	-	-	12.31	11.19	1.12	2.35	57.87	34.10	1.67	22.10	27.47	0.12
1-CeO_2	0.51	0.00	0.41	0.10	14.34	11.20	3.14	4.08	55.28	31.14	8.50	15.65	25.80	0.03
catalyst **A**	0.49	0.00	0.49	0.00	18.53	15.69	2.84	0.88	49.82	36.67	10.83	2.32	30.28	0.25

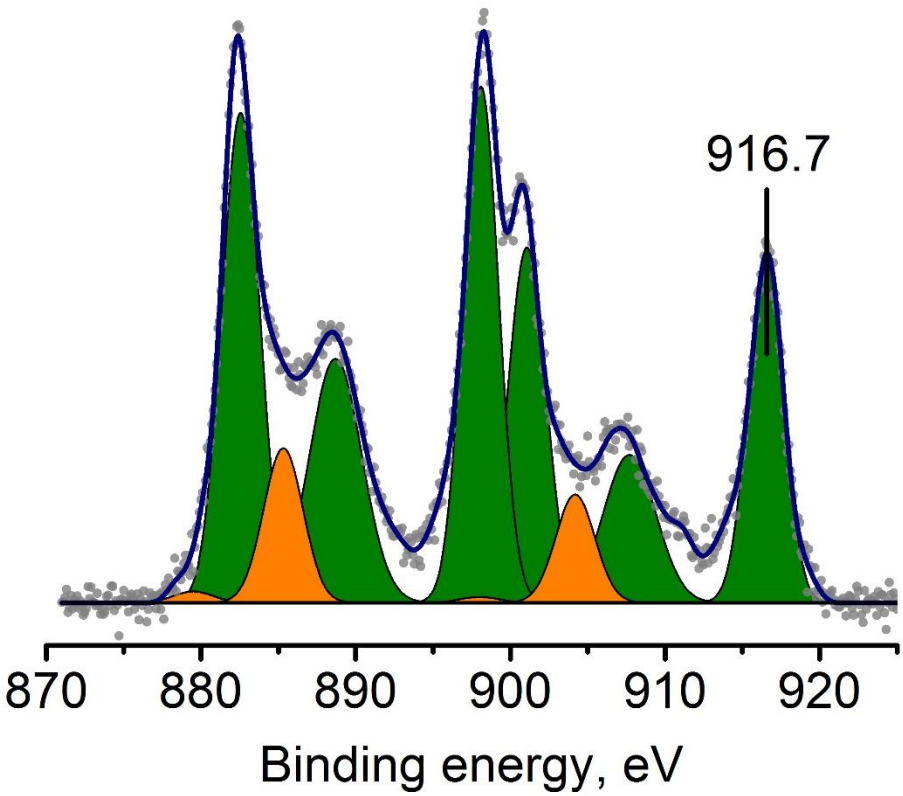

Figure S17. XPS analysis of Ce3d core level for the starting CeO_2.

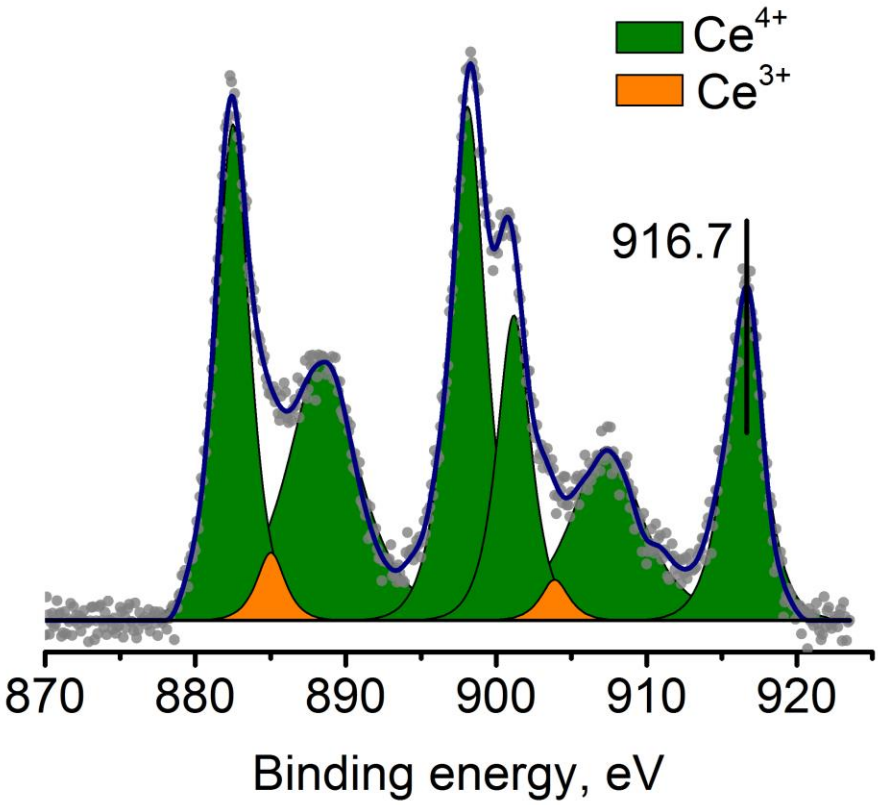

Figure S18. XPS analysis of Ce3d core level for the product **1**-CeO_2.

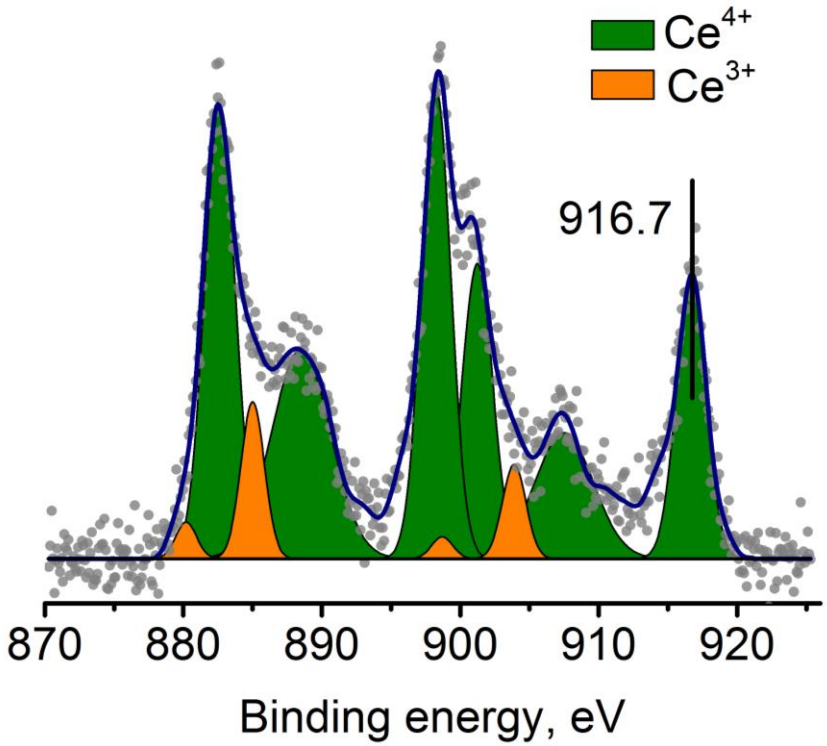

Figure S19. XPS analysis of Ce3d core level for catalyst **A**.

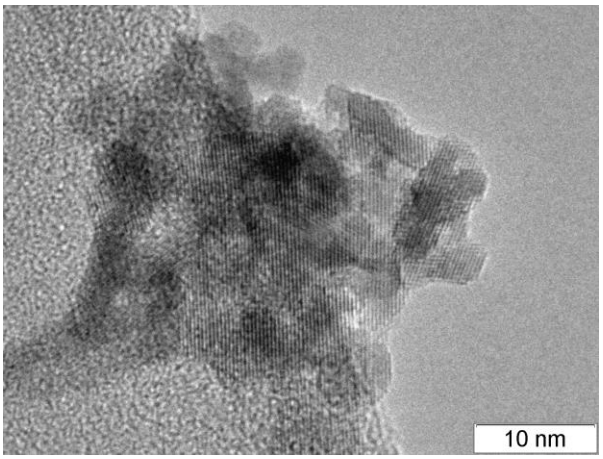
10 nm

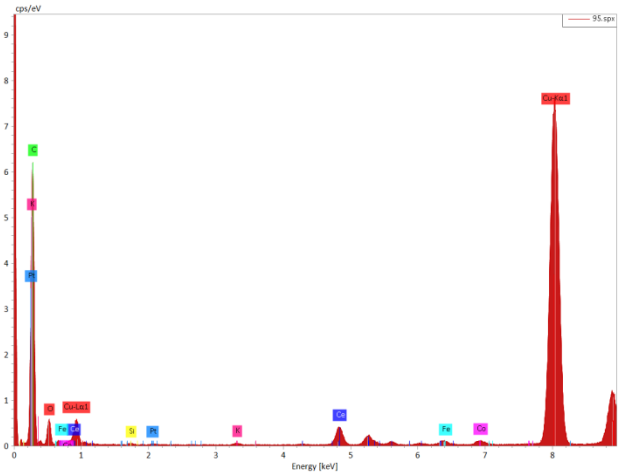
cps/eV
95.spx
Cu-Ka1
C
Ti
Pt
O
Cu-Ln1
Fe
Co
Si
Pt
Ti
Cr
Fe
Co
Energy [keV]

1

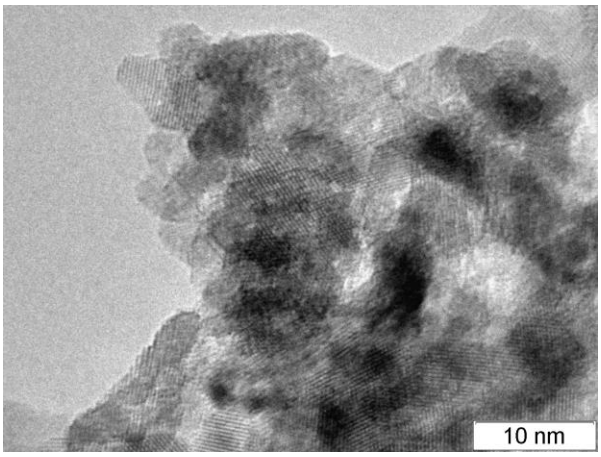
10 nm

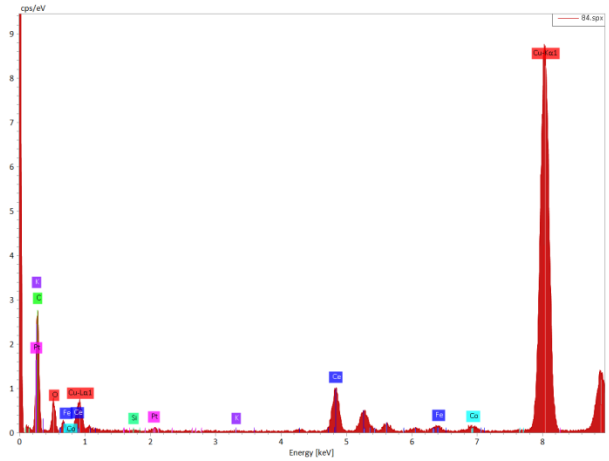
cps/eV
84.spx
Cu-Ka1
Ti
C
Pt
O
Cu-Ln1
Fe
Co
Si
Pt
Ti
Cr
Fe
Co
Energy [keV]

2

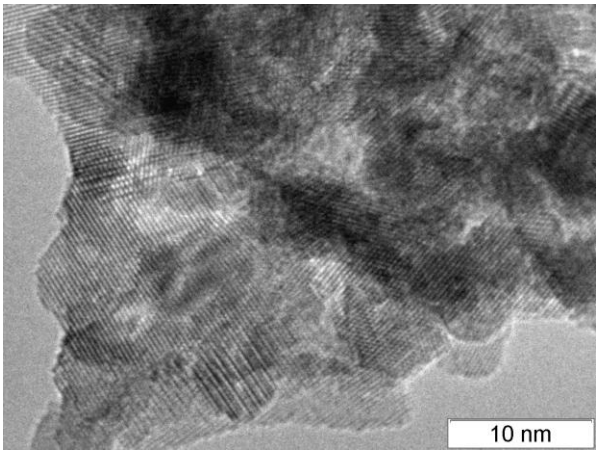
10 nm

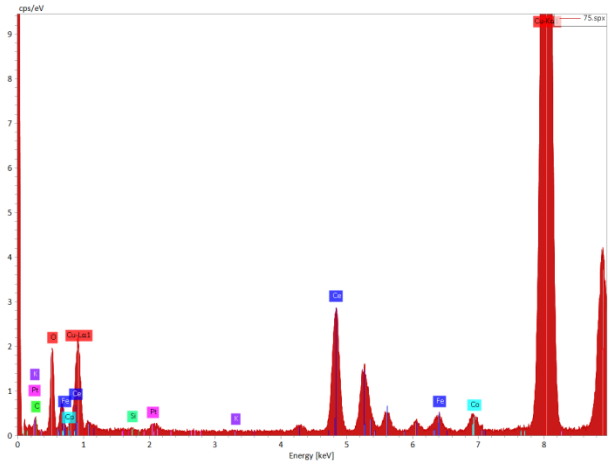
cps/eV
75.spx
Cu-Ka1
Cr
O
Cu-Ln1
Ti
Pt
C
Fe
Co
Si
Pt
Ti
Fe
Co
Energy [keV]

3

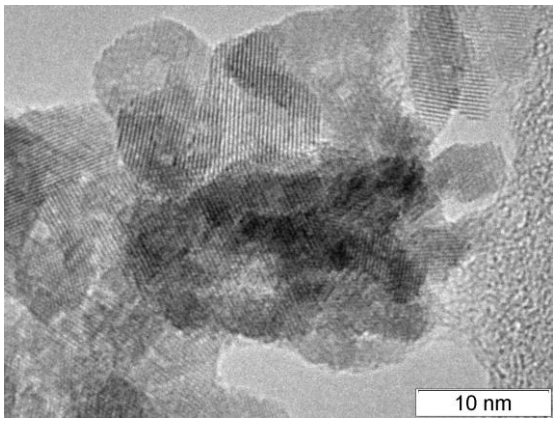

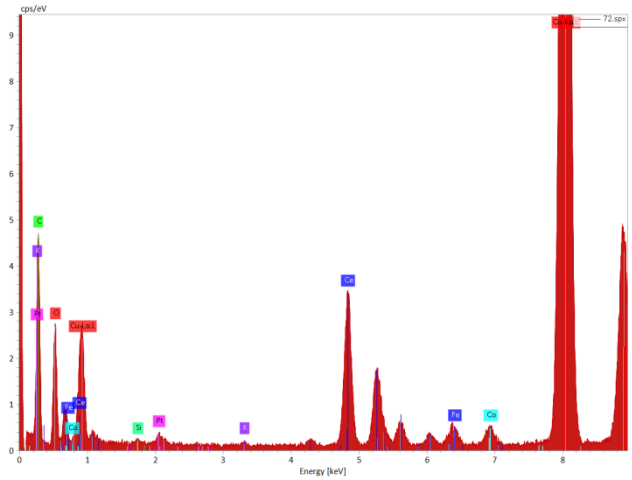

4

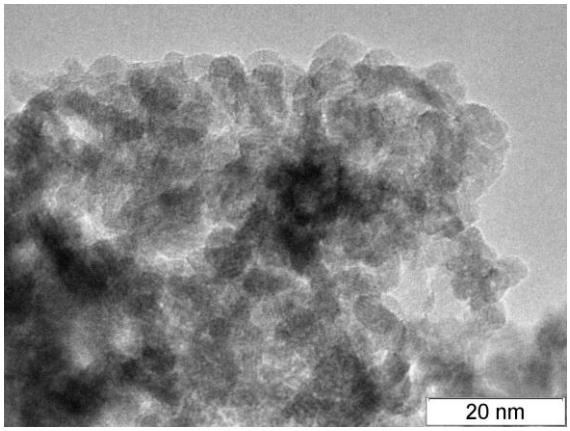

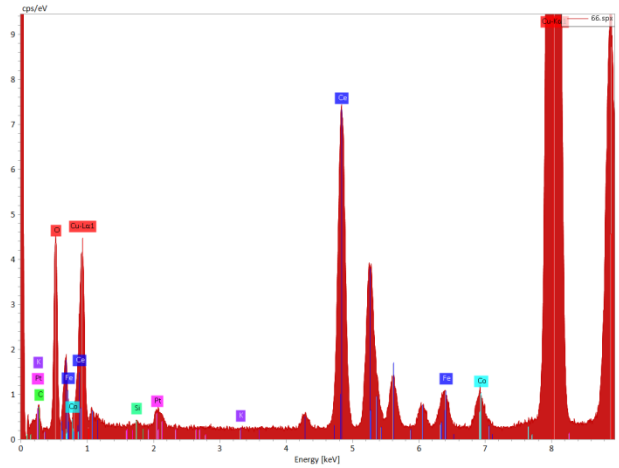

5

Figure S20. TEM images and EDX spectra of catalyst **A** taken from different area of the sample.

Table S13. Cerium and platinum atomic percentages in catalyst **A** calculated from EDX data taken from different area of the sample. Area numbers are the same as on the Figure S18:

Area	Cerium	Platinum
1	98.50	1.50
2	97.16	2.84
3	98.25	1.75
4	98.06	1.94
5	99.00	1.00
Mean	98.2±0.7	1.8±0.7

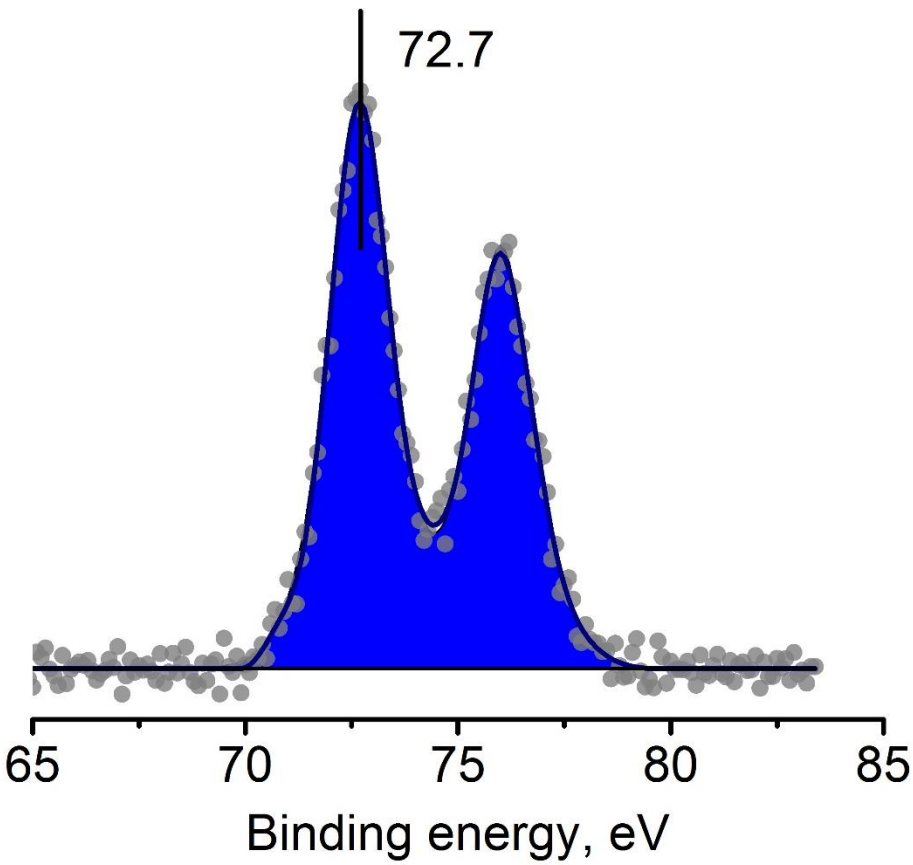

Figure S21. Curve-fitted XPS of the core level region of Pt(4f) of the catalyst **C** after the reaction.

Table S14. Atomic percentages and speciation in the catalyst **C** after the reaction calculated from XPS data.

	Atomic percentages and fraction of the species														
Sample	Pt	Pt^0	Pt^{2+}	Pt^{4+}	Cl	C	CC, CH	O-C=O	N	O	O-Ce	O-II	O-III	Ce	Ce^{3+} /Ce
catalyst **C**	0.87	0	0.47	0	4.67	26.25	24.20	2.05	0	38.61	32.88	3.28	2.45	29.59	0.07